

ORIGINAL ARTICLE

Improved delivery of doxorubicin by altering the tumor microenvironment using ultrasound combined with microbubbles and chemotherapy

Nina Xiao^{1,2}, Jianhua Liu^{1,2}, Lianlian Liao^{1,2}, Jimei Sun^{1,2}, Wenhui Jin^{1,2}, Xian Shu^{1,2}

¹Department of Medical Ultrasound, Guangzhou First People's Hospital, School of Medicine, South China University of Technology, Guangzhou, Guangdong, 510180, China; ²Department of Medical Ultrasound, Guangzhou First People's Hospital, Guangzhou, Medical University, Guangzhou 510180, China

Summary

Purpose: To determine whether low-intensity pulsed ultrasound (US) using microbubbles (MB) can temporarily promote regional blood flow in the tumor and increase the delivery of doxorubicin (ad).

Methods: We randomly divided 66 tumor-bearing rabbits into 6 groups (n=11/group). The 6 groups were as follows: doxorubicin and ultrasound combined with microbubble treatment group (Ad-US-MB treatment group), US-MB treatment group, US treatment group, MB treatment group, doxorubicin treatment group (Ad-treatment group), and control group. The animals were intravenously injected with doxorubicin hydrochloride; next, the tumors in the Ad-US-MB treatment group were subjected to low-intensity ultrasound with microbubbles for 10 min. Contrast-enhanced ultrasound (CEUS) imaging of tumor tissues was performed before and after the intervention. Next, we randomly selected 8 rabbits/group, which were euthanized immediately after treatment. The remaining

rabbits were reared and underwent the intervention every 7 days.

Results: Tumor perfusion increased immediately in the Ad-US-MB treatment group ($p < 0.01$). Unlike the Ad treatment group, the Ad-US-MB treatment group showed high levels of doxorubicin in the tumor samples ($p < 0.05$). Immunofluorescent staining showed high levels of doxorubicin mainly around the blood vessels; in addition, doxorubicin was observed in other areas in the Ad-US-MB treatment group. Inhibition of tumor growth was observed in the Ad-US-MB treatment group.

Conclusions: Low-intensity ultrasound combined with microbubbles and chemotherapy can alter the tumor microenvironment and temporarily increase the regional blood flow to the tumor.

Key words: doxorubicin, microbubbles, pulsed low-frequency ultrasound, tumor microvasculature, tumor microenvironment

Introduction

Cancer has been considered as a major public health issue because it may affect various tissues and organs of the body and continues to pose challenges for treatment. To date, cancer treatment mainly includes surgery, radiotherapy and chemotherapy. However, radiotherapy cannot be used to treat all types of cancer. The development of gene therapies and different kinds of supportive thera-

pies has established chemotherapy as a promising alternative method for targeting tumors.

The success of chemotherapy depends on targeted delivery to the cancer tissue. Targeted delivery of a chemotherapeutic agent depends on several factors governing the enhanced permeability and retention (EPR) effect [1], namely, regional blood flow to the tumor, permeability of

Correspondence to: Jianhua Liu, DM. Department of Medical Ultrasound, 5th Floor, Image Building, Guangzhou First People's Hospital, No. 1 Panfu Rd, Yuexiu District, Guangzhou Medical University, Guangzhou 510180, Guangdong, China
Tel: +86 20 81048075, Fax: +86 20 81048075, E-mail: cnjhdcc@126.com
Received: 05/06/2018; Accepted: 30/08/2018

the tumor vasculature, structural barriers imposed by the perivascular tumor cells and extracellular matrix, and intratumoral pressure. Previous studies [2-9] have shown that the tumor microvasculature is abnormal and lacks the conventional hierarchy of blood vessels. In addition to vascular heterogeneity, tumor blood vessels have structural abnormalities. The endothelial surface of the blood vessels of the tumor is fenestrated with gaps between the endothelial cells with no or abnormal basement membrane and few or poorly adherent pericytes. Therefore, chemotherapeutic drugs with long circulation times preferentially leak into the tumor tissue through the leaky tumor vasculature, and thus are retained in the tumor bed because of reduced lymphatic drainage. A decrease in the lymphatic drainage and mechanical compression of downstream blood vessels due to tumor cell proliferation increases the level of interstitial fluids in the tumor. Furthermore, blood perfusion in the tumor tissue is significantly lower than that in the surrounding normal tissue owing to the leakiness and/or compression of the blood vessels of the tumor. Impaired perfusion reduces oxygen supply and results in a hypoxic microenvironment. Hypoxia promotes the proliferation of tumor cells, cells of the extracellular matrix (ECM) and different types of stromal cells, and thus increases the pressure on the blood and lymphatic vessels. Consequently, blood flow to the tumor is impaired, lymphatic drainage is reduced and the interstitial

pressure in the tumor is increased. High interstitial pressure inhibits the accumulation of drugs in the tumor. Therefore, restoring the microenvironment and blood vessels of the tumor is an efficient strategy for chemotherapeutic drug delivery.

We aimed to increase the delivery of the chemotherapeutic drug by altering the tumor microenvironment and temporarily increasing the regional blood flow to the tumor. Vascular effects induced by low-intensity pulsed ultrasound combined with microbubbles can significantly increase the tumor blood perfusion (Figure 1). Some authors [11] suggest that ultrasound-microbubble (US-MB) interactions temporarily stimulate neovascularization in the gracilis muscle of rats as an inflammatory reaction. Activation by low-intensity ultrasound-microbubble (US-MB) interactions triggers the inflammatory reaction. Low-intensity ultrasound irradiation significantly improved limb perfusion and revascularization in animal models with limb ischemia. Under certain conditions, ultrasonic MB destruction creates arteriogenesis and angiogenesis in skeletal muscles. In skeletal muscles affected by arterial occlusion, arteriogenesis and hyperemia can be significantly enhanced by ultrasonic MB destruction [10-13].

Methods

The study was approved by the Animal Research Committee of the Guangzhou First Municipal People's Hospital and was conducted in accordance with the NIH Guide for the Care and Use of Laboratory Animals.

Animal model

Healthy New Zealand white rabbits of 2.5 kg were obtained from the experimental center in Guangdong, China. All the rabbits were reared at temperatures of 24–26°C and humidity of 45–55%. Before inoculation, all the rabbits were reared in the environment for at least 7 days.

The VX2 tumor tissue suspension was obtained from the cell bank of Sun Yat-sen University (Guangzhou, China). The tumor tissues were chopped into small chunks (1 mm³) using Ophthalmic scissors and placed in a culture dish with normal saline solution. The suspension was subcutaneously injected in the superficial muscle of the left hind limb of anesthetized rabbits. The experiment was performed 7 days after tumor implantation when a tumor diameter of approximately 10 mm was achieved.

Experimental procedures

We randomly divided the 66 tumor-bearing rabbits into 6 groups (n = 11/group). The 6 groups were as follows: doxorubicin therapy together with ultrasound combined with microbubble treatment group (Ad-US-MB treatment group), US-MB treatment group, US treat-

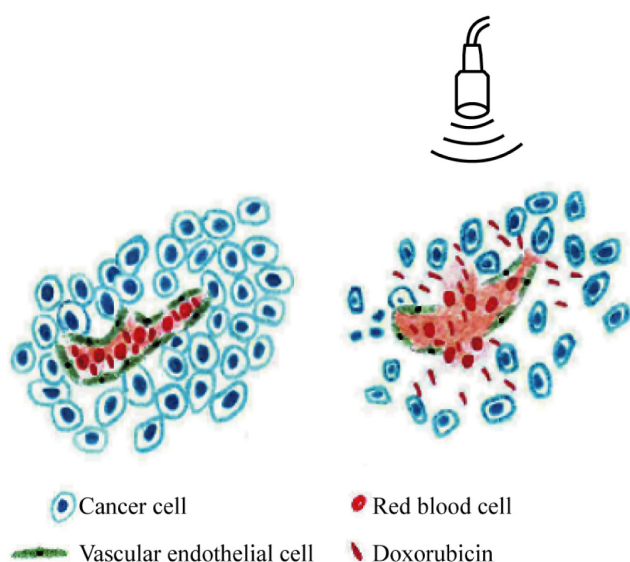


Figure 1. Effect of ultrasound and microbubbles on tumor microenvironment. Chemotherapy in the presence of microbubbles and low-frequency ultrasound has influenced the solid stress around the tumor microvessels. There was microvascular congestion and expansion, the shape of the vessel is round or oval, the structure of the wall is not complete and leakage of red blood cells can be seen.

ment group, MB treatment group, doxorubicin treatment group (Ad-treatment group), and control group. All the study animals were anesthetized by intramuscular injection of xylazine hydrochloride (0.15 mL/kg, Shengda Animal Pharmaceuticals Co., Ltd., Xinchun Lane 1, Danjiang St., Dunhua, Jilin, China) and 2% pentobarbital sodium (20 mg/kg, No.69, the 2nd St., Huangjing building, Jinjiang District, Chengdu, China). Subsequently, all groups were established with intravenous access and contrast-enhanced ultrasound (CEUS) was performed.

Animals in the Ad-US-MB treatment group were intravenously injected with doxorubicin hydrochloride at a concentration of 2 mg/mL at a dose of 6 mg/kg [14-16] (Wanle pharmaceutical building, Shenzhen national Biomedicine industry Base, Lanzhu Road, Pingshan Dist., Shenzhen, China). Next, the tumor was subjected to low-intensity ultrasound irradiation and microbubbles at a dosage of 0.1 ml/kg (Department of Ultrasound, Xinqiao Hospital Affiliated to Third Military Medical University, Chongqing, China) for 10 min for temporarily increasing the permeability of the blood-tumor barrier. Animals in the US-MB treatment group were intravenously injected with the same volume of saline solution as that of the doxorubicin solution, and then the tumor was subjected to low-intensity ultrasound irradiation and microbubbles for 10 min. Animals in the US treatment group were intravenously injected with the same volume of saline solution, and then the tumor was subjected to low-intensity ultrasound irradiation for 10 min. Animals in the MB treatment group were intravenously injected with the same volume of saline solution followed by an intravenous injection with the same volume of microbubbles. The tumor of the animals in this group was subjected to sham ultrasound irradiation for 10 min. Animals in the Ad treatment group were intravenously injected with doxorubicin hydrochloride, and then were intravenously injected with the same volume of saline solution; the tumor of the animals in this group was subjected to sham ultrasound irradiation for 10 min.

CEUS was performed in all groups and the peak intensity was analyzed. We randomly selected 8 rabbits/group, which were euthanized immediately after treatment. The tumor tissue was divided into two equal parts. One part of the tumor tissue was randomly selected to determine the concentration of doxorubicin using fluorometric analysis. The other tissue sample was subjected to hematoxylin and eosin (H&E) staining and immunofluorescence staining. The remaining rabbits were reared for 28 days after the first intervention and were administered the respective interventions every 7 days. The growth of the rabbits was monitored using the ultrasound system operating in B-mode.

B-mode and CEUS perfusion imaging

CEUS is a non-invasive and reliable imaging method for determining tumor perfusion [17]. Ultrasound imaging in the B-mode and CEUS imaging were performed using an ultrasound system with an L12-5 transducer of the Philips IU22 (Royal Dutch Philips Electronics Ltd., Amsterdam, Netherlands). Lipid-shelled perfluoropropane microbubbles were prepared using the high-speed

shearing method. The rabbits were anesthetized and placed in ventral recumbency. An initial B-mode imaging was performed at a mechanical index of 0.07. After the intravenous injection of microbubbles at a dose of 0.01 mL/kg in the ear vein of rabbits, CEUS perfusion imaging was performed with contrast pulse sequencing at a centerline frequency of 12 MHz and a mechanical index of 0.08. A time-intensity curve of contrast signals was then plotted and the peak intensity value was used for comparisons.

Tumor volume was assessed every 7 days for 28 days using B-mode ultrasound imaging at a mechanical index of 0.08. In each of the B-mode images, the length (L) and width (W) of the tumor were measured. Tumor volume (V) was then calculated as follows: $\pi \times (L \times W^2) / 6$ [18].

Low-intensity ultrasound treatment

Treatment was performed using a pulsed-ultrasound device with a KHT-017 transducer (DCT-700; Shenzhen Well. D Medical Electronic, Shenzhen, China). To maintain a distance of 2 cm between the transducer and the skin overlying the tumor, the transducer was fixed on a steel stand with a scale. Subsequently, ultrasound coupling gel was applied to the skin. To avoid the interference of microbubbles in the CEUS, treatment was commenced 15 min after the first CEUS and lasted for about 10 min [19]. The US-MB treatment was applied to the tumor after intravenous injection of microbubbles at a dose of 0.1 mL/kg. The transducer was operated at a frequency of 1 MHz, acoustic pressure of 1 Mpa, the pulse repetition frequency of 10 Hz, and a duty cycle of 0.2%. The treatment was performed using an intermittent mode of 9 s on and 3 s off for 10 min.

H&E staining

Formalin-fixed paraffin-embedded serial sections of the tumor tissue were used for H&E staining to assess the therapeutic effect in each group. We randomly selected 10 fields of vision using an optical microscope (Axio Scope A1, ZEISS, Oberkochen, Germany). We performed optical microscopy at high power to observe the changes in tumor cells and tumor microvessels.

Fluorometric analysis

We used the 960MC fluorescence spectrophotometer to detect the concentration of doxorubicin in tumor tissues using silver nitrate (AgNO₃) spectrofluorimetry [20]. The frozen tissues were weighed and homogenized in a blender (5 min) with 1 mL double distilled water. We added 1 mL of the tissue sample to tubes containing 0.2 mL 33% AgNO₃ and the tubes were shaken vigorously for 10 min at 4°C. Then, we added 4 mL pre-cooling isoamyl alcohol to the tube. The suspension was centrifuged at 4500 r/min for 15 min. The precipitate was removed, and the clear supernatant was used to determine fluorescence intensity. Excitation wavelength and emission wavelength were set at 490 and 560 nm. The concentration of doxorubicin was determined by drawing a standard curve.

Immunofluorescence staining

Doxorubicin autofluorescence was detected using a Nikon Eclipse C1 fluorescence microscope with a 100 W HBO mercury light source equipped with a 510 to 560 nm excitation and a 590-nm emission filter set. Tissue sections were imaged with a Nikon DS-U3 image-forming system. Blood vessels in tissue sections were recognized by the expression of CD31 on endothelial cells. Subsequent to imaging of doxorubicin, tissue sections were fixed in paraformaldehyde for 10 min. Then, the sections were washed in phosphate-buffered saline (PBS) and blocked with a protein-blocking reagent (BSA) for 30 min to prevent non-specific antibody binding. The

sections were stained with a rat anti-CD31 (1/300) antibody cocktail for 12 h in a humidified chamber (antibody dilutions indicated in parentheses). Further, the sections were washed in PBS and stained with a Cy3-conjugated goat anti-rat IgG secondary antibody (1/200) for 50 min to recognize the rat anti-CD31 antibody. Sections were washed in PBS and were incubated with the 4',6-diamidino-2-phenylindole (DAPI) dye in the dark at room temperature for 10 min. Then, the sections were washed in PBS and air-dried for fluorescent imaging. Tissue sections were re-imaged according to the same method used to capture doxorubicin fluorescence. The fluorescence of blood vessels was green, that of tumor cell nuclei blue and that of doxorubicin red [15,16].

Statistics

Multiple comparisons were performed using one-way analysis of variance (ANOVA) followed by a Bonferroni correction. The paired samples *t*-test was used to compare differences before and after treatment in each group. Comparisons of tumor volume between two groups were performed using repeated measures ANOVA. Data were expressed as mean ± standard deviation and *p*<0.05 was considered to indicate statistical significance. Statistical analyses were performed using SPSS20.0 (IBM SPSS, Chicago, IL).

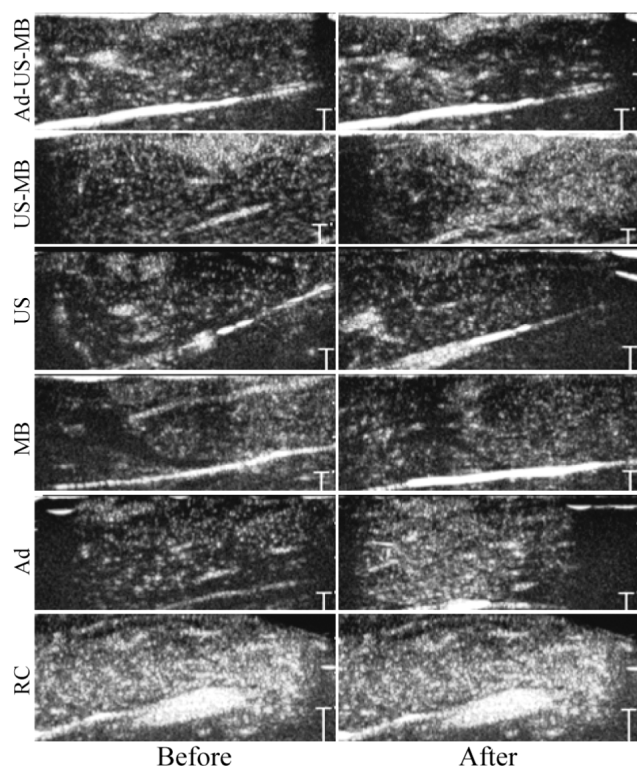


Figure 2. CEUS perfusion imaging. The visual strength of CEUS in Ad-US-MB treatment group was slightly stronger than that before treatment. No significant change before and after treatment was noted in Ad, US and MB treatment groups and BC treatment group.

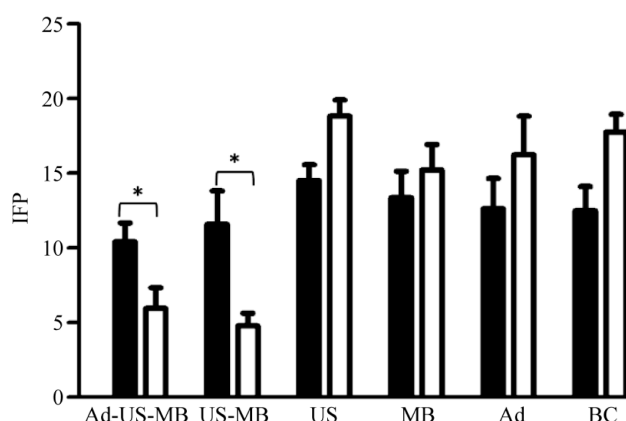


Figure 3. In the Ad-US-MB treatment group, tumor peak intensity perfusion (PI) increased immediately after treatment (**p*=0.003). The PI change in the US-MB, US, MB, Ad and BC treatment groups had no statistical significance.

Table 1. The peak intensity of CEUS perfusion imaging

Group	Trt before		Trt after		Trt diff		P for inner group
	Mean	SD	Mean	SD	Mean	SD	
Ad-US-MB	14.55	4.14	16.22	3.89	1.66	1.03	0.003
US-MB	14.39	3.25	16.06	3.31	1.66	2.52	0.104
US	17.42	3.58	16.50	5.40	-0.92	2.83	0.390
MB	15.09	5.46	13.40	1.99	-1.69	6.77	0.502
Ad	14.79	4.20	15.78	3.68	1.00	6.85	0.693
BC	13.31	2.75	14.26	2.42	0.94	1.89	0.201
P for group	0.470		0.459		0.459		

For abbreviations see text

Results

The effects of various treatments on tumor perfusion

Tumor perfusion increased immediately after treatment in the Ad-US-MB treatment group ($p < 0.01$; Figures 2 and 3 and Table 1). Tumor perfusion did not change significantly in the remaining treatment groups. H&E staining showed disruption of the tumor microvessels immediately after treatment in the Ad-US-MB treatment group. The degree of microvessel injury was mild, as evidenced by vasodilation, congestion, and hemorrhage (Figure 4).

H&E staining

The US, MB and control groups showed similar H&E staining results. Irregular nests were observed in the tumor tissue. We observed tumor cells in different stages of proliferation; the tumor cells were in the nest configuration, were densely arranged, and their large nuclei were stained. No obvious injury to be blood vessel wall was observed, and

red blood cells (RBCs) were present within the lumen. Focal necrosis of tumor cells was observed in the Ad group and US-MB group. The US-MB group showed congestion and expansion of blood vessels, the shape of the vessel was round or oval, the structure of the vessel wall was discontinuous and leakage of RBCs was observed. The US-MB-Ad group showed results similar to those observed in the US-MB group (Figure 4).

The concentration and distribution of doxorubicin

We investigated the mechanisms underlying the effect of ultrasound combined with microbubbles on the accumulation of doxorubicin. Compared to the Ad group, the Ad-US-MB group showed increased tissue accumulation of doxorubicin ($p < 0.05$; Table 2 and Figure 5). The relationship between the fluorescence of blood vessels, doxorubicin, and tumor cells is shown in Figure 6. The fluorescence of blood vessels was green, that of tumor cell nuclei blue, and that of doxorubicin red (Figure 6). The tumors showed heterogeneous vascularization. High concentrations of doxorubi-

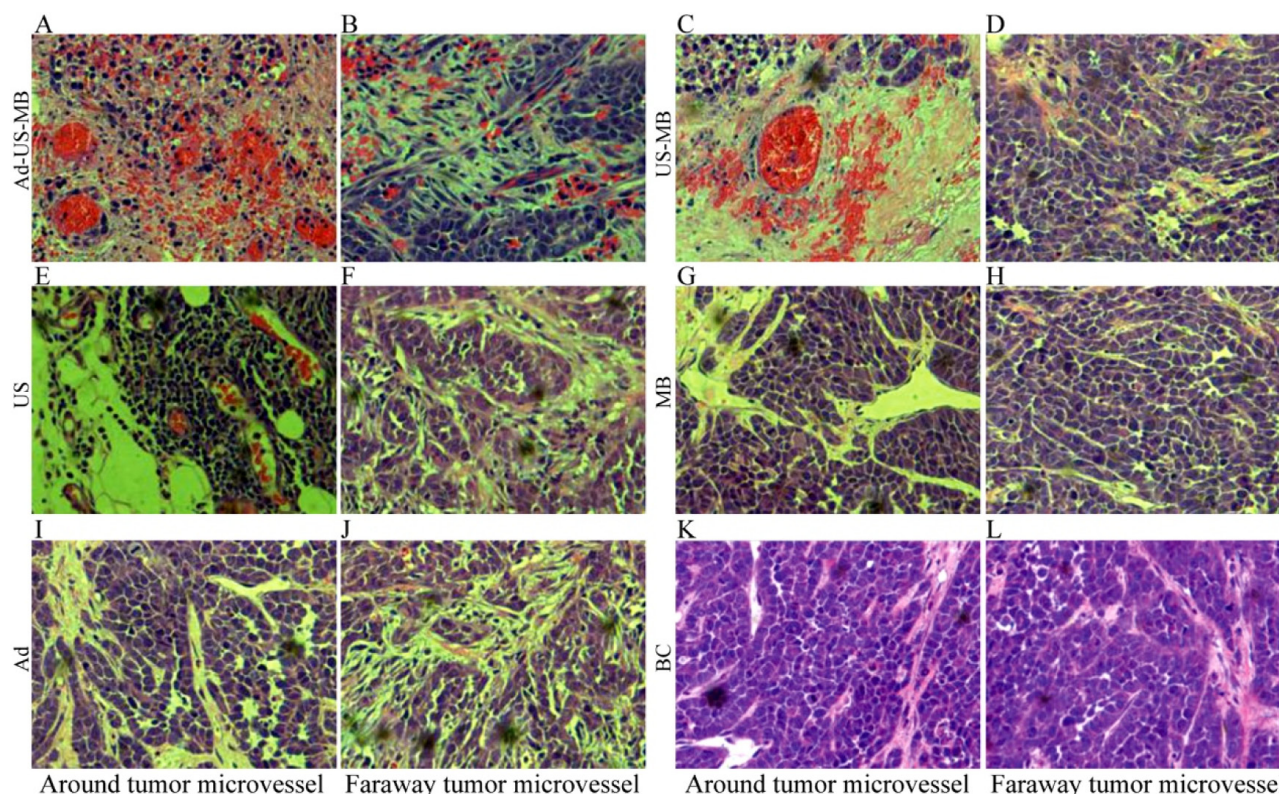


Figure 4. H&E staining: In the US-MB-Ad and US-MB groups, focal necrosis of tumor cells was found also, microvascular congestion and expansion occurred, the shape of the vessel is round or oval, leakage of red blood cells can be seen around and far away from the tumor microvessels. The pathological results are basically the same in the US, MB and BC groups. The shape of microvessels is irregular and their construction is distorted. The microvessels have no obvious wall injury, there are no red blood cells around and far away from the tumor microvessels. Focal necrosis of tumor cells was observed in the Ad group and US-MB group. The US-MB groups showed congestion and expansion of blood vessels, the shape of the vessel was round or oval, the structure of the vessel wall was discontinuous and leakage of RBCs was observed. The US-MB-Ad group showed results similar to those observed in the US-MB group.

bicin were observed mainly around the blood vessels; in addition, doxorubicin was observed at the edge of tumor margins in the Ad-US-MB treatment group (Figure 6A). Relatively low concentrations of doxorubicin were observed around the blood vessels in the Ad treatment group whereas avascular and adjacent regions of the tumor did not contain detectable levels of doxorubicin. In addition, a small number of blood vessels did not contain any doxorubicin (Figure 6B). Therefore, our results indicated that ultrasound combined with microbubble therapy increases the vascular permeability of particles into the tumor interstitium.

Table 2. The concentration of Ad in the two groups (mean±SD)

Group	The concentration of Ad	Z	P
Ad-US-MB	0.682±0.000	-1.995	0.046
Ad	0.422±0.357		

For abbreviations see text

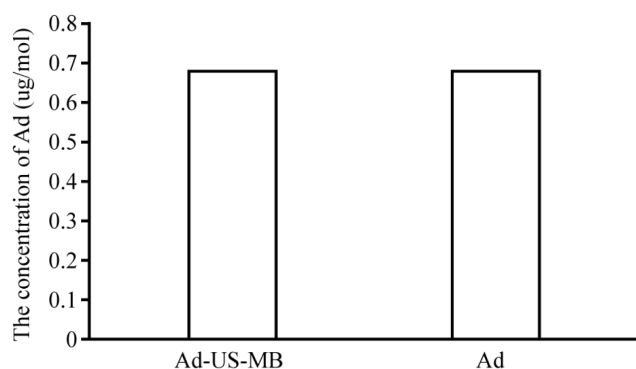


Figure 5. The concentration of doxorubicin in samples from the Ad-US-MB treatment group is higher than the concentration of doxorubicin in the Ad treatment group. The difference was statistically significant ($p=0.046$).

Sensitivity of tumors to various treatments

The growth of tumors in all treatment groups is shown in Figure 7. A delay in tumor growth is expressed as the treatment duration in the Ad-US-MB and Ad treatment groups compared to that in the other groups. An increase in the duration of treatment significantly decreased the volume in the tumor in the Ad-US-MB and Ad treatment groups. The tumor volume of the Ad-US-MB treatment group was lower than that in the Ad treatment group 24 days after treatment.

Discussion

Tumor growth and progression produce solid stress. This stress compresses the blood and lymphatic vessels, reducing the perfusion rates and creating hypoxia. Solid and fluid stress constitute the physical force exerted by the tumor [3,4]. Solid stress, the mechanical forces exerted by non-fluid components of the tumor, increases with an increase in the proliferation of tumor cells and strains the tumor microenvironment thus deforming the surrounding normal tissue. The solid stress that remains in the tissue after it is excised and external loads are removed is referred to as growth-induced or residual stress. Solid stresses affect the tumor pathophysiology in at least two ways: directly by compressing the cancer and stromal cells and indirectly by deforming the blood and lymphatic vessels. Cell compression alters gene expression, cancer cell proliferation, apoptosis, invasiveness, stromal cell function, ECM synthesis and organization. Blood and lymphatic vessel compression reduces the delivery of oxygen, nutrients, and drugs, creating a hypoxic and acidic microenvironment

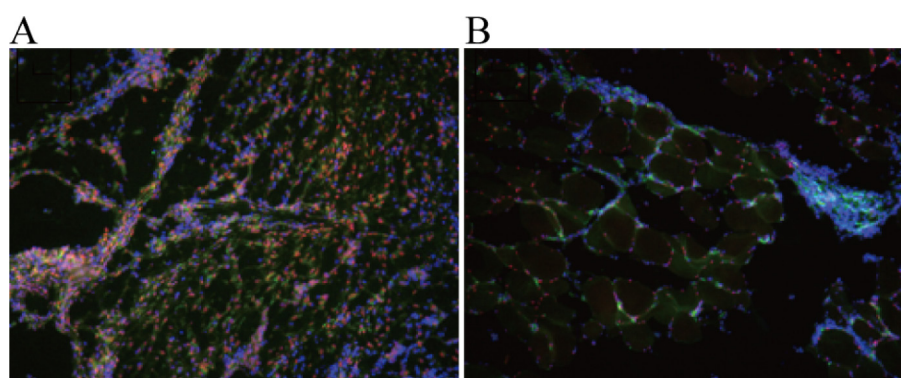


Figure 6. Immunofluorescence staining shows the relationship between tumor blood vessels, doxorubicin and tumor cells. Blood vessels were indicated as green, tumor cell nuclei were indicated as blue, whereas doxorubicin autofluoresced red. High concentrations of doxorubicin were observed mainly around blood vessels, and were even discovered at the edge of tumor margins in the Ad-US-MB treatment group (A), while relatively low concentrations of doxorubicin were observed only around blood vessels in the Ad treatment group, avascular and adjacent regions of the tumor did not contain detectable doxorubicin. Also, there were a small number of blood vessels without surrounding doxorubicin (B). **A:** Ad-US-MB, **B:** Ad.

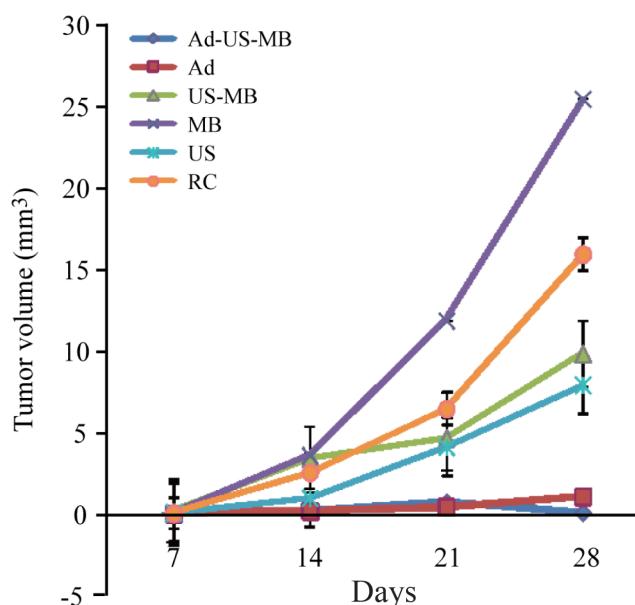


Figure 7. Tumor growth curve. Tumor growth delay is expressed as treatment continued in the Ad-US-MB and Ad treatment groups compared with the other groups. As treatment continued, the tumor volume significantly reduced in the Ad-US-MB and Ad treatment groups. Nevertheless, tumor volume in the Ad-US-MB treatment groups was smaller than that in the Ad treatment group 24 days after treatment.

and compromising therapeutic outcomes. Fluid stress consists of the forces exerted by the fluid components of the tumor, including the microvascular and interstitial fluid pressures, as well as the shear stress exerted by blood and lymphatic flow on the vessel wall and by the interstitial flow on cancer and stromal cells and the ECM [21,22]. Fluid stresses are determined in large part by the combined effect of the structure of tumor vessels and the compression of blood and lymphatic vessels. Blood vessel compression reduces the effective “flow” cross-section of the vessel and thus increases the resistance to blood flow, which can affect perfusion.

In this study, we designed and performed a series of comparative in vivo experimental observations, including assessments of blood perfusion, microvessel morphology, and tumor levels of the chemotherapeutic drug. CEUS perfusion imaging showed that tumor perfusion increased immediately after treatment in the Ad-US-MB group. However, tumor perfusion did not increase immediately as expected after treatment in the US-MB group. The interactions between US and MBs are not sufficient to improve the tumor microenvironment. Tumor perfusion and delivery of doxorubicin increased in the Ad-US-MB treatment group. Our results indicate that Ad-US-MB can improve the tumor microenvironment and microvasculature.

Doxorubicin is a traditional chemotherapeutic drug. Therapeutic strategies to improve perfusion include vascular normalization and vascular decompression by alleviating the solid stress inside tumors. Doxorubicin not only decreases the cell compression but also decreases the blood and lymphatic vessel compression. Moreover, doxorubicin alleviates the solid stress in tumors. Previous studies have shown that pharmacological agents modify the tumor microenvironment or improve tumor penetrability [23,24]. US-MB decreases the interstitial pressure in the tumor and degrades the ECM [25]. Degradation of the ECM not only alleviates the lymphatic vessel compression but also the vascular compression. Vascular decompression restores the shape of blood vessels and improves microvessel perfusion. Ad-US-MB treatment may improve the tumor microenvironment. Therefore, blood perfusion in tumors may be temporarily increased, thus increasing the therapeutic effect of the chemotherapeutic drug.

Chemotherapy in the presence of microbubbles and low-intensity ultrasound increases the in vivo delivery of the agent to a tumor and minimizes harmful systemic side effects in normal tissues. Previous studies indicate that low-intensity ultrasound combined with microbubbles can temporarily increase the permeability of the blood-brain barrier (BBB) [26-30], thereby allowing the passage of chemotherapeutic agents into the neural tissue, which is of particular relevance in cancer therapy. The use of ultrasound to permeabilize the vascular endothelium and cellular membranes is referred to as sonoporation, which is known to profit substantially from the concomitant use of microbubbles [31-33]. The underlying bio-effect of insonation is cavitation [34]. The sound pressures from cavitating microbubbles cause transient increase in the permeability of the cell membranes, allowing exogenous molecules such as chemotherapeutic agents to enter the cell [35-39]. Further, the intracellular delivery of therapeutic compounds may be facilitated by endocytosis and pore formation involving the endothelial cells lining blood vessels [16]. Low-intensity ultrasound combined with microbubble treatment may injure the vascular endothelial cells and increase the gap between the endothelial cells; therefore, the permeability of the vessels and the extravasation of RBCs into the interstitial space of the tumor is increased. We did not observe necrosis in our study. In the US-MB-Ad group, we observed focal necrosis of tumor cells, congestion and expansion of the microvasculature, round- or oval-shaped vessels, abnormal vessel wall structure, and leakage of RBCs. Thus, our findings indicate that chemotherapy and low-intensity ultra-

sound with microbubbles may improve the tumor microenvironment.

Mild injury to the blood vessel by cavitation may improve the permeability of the vessel and drug delivery. The biological effects include sonoporation, widening of the cell gap and changes in vessel architecture. Most of the vessel injuries recover after some time. US-MB treatment alters the cell morphology and creates a pore on the cell membrane, a process known as sonoporation. Under different parameters, the cell membrane may form different size pores from dozens of nanometers to hundreds of nanometers; the passage of particles of different sizes can be regulated by adjusting the parameters. Sonoporation uses ultrasound to generate transient non-selective pores on the cell membrane and increase drug and gene delivery. The pores of the cell membrane may rapidly seal in microseconds to a few seconds. Thus, the cell is alive after the sealing of the cell membrane pores [40,41]. Our results indicate that tumor perfusion and delivery of doxorubicin increased with an increase in the interaction of Ad, US and MB. This shows that low-intensity pulsed ultrasound combined with microbubbles can be used as a means of sensitizing clinical chemotherapy and can be

used in combination with chemotherapy. The effect of the combination treatment can be improved by altering the ultrasound parameters, including acoustic pressure, frequency, pulse repetition frequency, duty cycle, and intermittent mode, when using different chemotherapeutic agents.

Conclusion

Our results showed that ultrasound combined with microbubbles and chemotherapy could be used to alter the tumor microenvironment for increasing drug accumulation in tumors.

Acknowledgements

This work was funded by Guangdong Natural Science Foundation: Ultrasound and microbubbles modulate tumor blood flow and enhance the efficacy of chemotherapy in hypovascular tumors (Contract no. 2016A030313461).

Conflict of interests

The authors declare no conflict of interests.

References

1. Kobayashi H, Watanabe R, Choyke PL. Improving conventional enhanced permeability and retention (EPR) effects; what is the appropriate target? *Theranostics* 2013;4:81-9.
2. Chauhan VP, Martin JD, Liu H et al. Angiotensin inhibition enhances drug delivery and potentiates chemotherapy by decompressing tumour blood vessels. *Nat Commun* 2013;4:2516.
3. Stylianopoulos T, Martin JD, Chauhan VP et al. Causes, consequences, and remedies for growth-induced solid stress in murine and human tumors. *Proc Natl Acad Sci U S A* 2012;109:15101-8.
4. Jain RK, Martin JD, Stylianopoulos T. The role of mechanical forces in tumor growth and therapy. *Annu Rev Biomed Eng* 2014;16:321-6.
5. Stylianopoulos T, Jain RK. Combining two strategies to improve perfusion and drug delivery in solid tumors. *Proc Natl Acad Sci U S A* 2013;110:18632-7.
6. Dudley AC. Tumor endothelial cells. *Cold Spring Harb Perspect Med* 2012;2:a006536.
7. Jain RK. Normalizing tumor microenvironment to treat cancer: bench to bedside to biomarkers. *J Clin Oncol* 2013;31:2205-18.
8. Martin JD, Fukumura D, Duda DG, Boucher Y, Jain RK. Corrigendum: Reengineering the Tumor Microenvironment to Alleviate Hypoxia and Overcome Cancer Heterogeneity. *Cold Spring Harb Perspect Med* 2016;6:a031195.
9. Goel S, Duda DG, Xu L, Munn LL, Boucher Y, Fukumura D, Jain RK. Normalization of the vasculature for treatment of cancer and other diseases. *Physiol Rev* 2011;91:1071-1121.
10. Johnson CA, Sarwate S, Miller RJ, O'Brien WD Jr. A temporal study of ultrasound contrast agent-induced changes in capillary density. *J Ultrasound Med* 2010;29:1267-75.
11. Chappell JC, Klibanov AL, Price RJ. Ultrasound-microbubble-induced neovascularization in mouse skeletal muscle. *Ultrasound Med Biol* 2005;31:1411-22.
12. Barzelay S, Sharabani-Yosef O, Holbova R et al. Low-intensity ultrasound induces angiogenesis in rat hind-limb ischemia. *Ultrasound Med Biol* 2006;32:139-45.
13. Chappell JC, Song J, Klibanov AL, Price RJ. Ultrasonic microbubble destruction stimulates therapeutic arteriogenesis via the CD18-dependent recruitment of bone marrow-derived cells. *Arterioscler Thromb Vasc Biol* 2008;28:1117-22.
14. Primeau AJ, Rendon A, Hedley D, Lilje L, Tannock IF. The distribution of the anticancer drug Doxorubicin in relation to blood vessels in solid tumors. *Clin Cancer Res* 2005;11:8782-8.

15. Li T, Wang YN, Khokhlova TD et al. Pulsed High-Intensity Focused Ultrasound Enhances Delivery of Doxorubicin in a Preclinical Model of Pancreatic Cancer. *Cancer Res* 2015;75:3738-46.
16. Zhao S, Yu H, Du N. Experimental study of doxorubicin interventional chemotherapy in the treatment of rabbit VX2 renal transplantation carcinoma. *Int J Clin Exp Med* 2015;8:10739-45.
17. Forsberg F, Ro RJ, Potoczek M et al. Assessment of angiogenesis: implications for ultrasound imaging. *Ultrasonics* 2004;42:325-30.
18. Leite de Oliveira R, Deschoemaeker S, Henze AT et al. Gene-targeting of phd2 improves tumor response to chemotherapy and prevents side-toxicity. *Cancer Cell* 2012;22:263-77.
19. Wang J, Zhao Z, Shen S et al. Selective depletion of tumor neovasculature by microbubble destruction with appropriate ultrasound pressure. *Int J Cancer* 2015;137:2478-91.
20. Schwartz HS. A fluorometric assay for daunomycin and adriamycin in animal tissues. *Biochem Med* 1973;7:396-404.
21. Baxter LT, Jain RK. Transport of fluid and macromolecules in tumors. I. Role of interstitial pressure and convection. *Microvasc Res* 1989;37:77-104.
22. Oldberg A, Kalamajski S, Salnikov AV et al. Collagen-binding proteoglycan fibromodulin can determine stroma matrix structure and fluid balance in experimental carcinoma. *Proc Natl Acad Sci USA* 2007;104:13966-71.
23. Jain RK. Normalization of tumor vasculature: an emerging concept in antiangiogenic therapy. *Science* 2005;307:58-62.
24. Goins B, Phillips WT, Bao A. Strategies for improving the intratumoral distribution of liposomal drugs in cancer therapy. *Expert Opin Drug Deliv* 2016;13:873-89.
25. Watson KD, Lai CY, Qin S et al. Ultrasound increases nanoparticle delivery by reducing intratumoral pressure and increasing transport in epithelial and epithelial-mesenchymal transition tumors. *Cancer Res* 2012;72:1485-93.
26. Wood AK, Sehgal CM. A review of low-intensity ultrasound for cancer therapy. *Ultrasound Med Biol* 2015;41:905-28.
27. Lammers T, Koczera P, Fokong S et al. Theranostic USPIO-Loaded Microbubbles for Mediating and Monitoring Blood-Brain Barrier Permeation. *Adv Funct Mater* 2015;25:36-43.
28. Hynynen K. Ultrasound for drug and gene delivery to the brain. *Adv Drug Deliv Rev* 2008;60:1209-17.
29. Vlachos F, Tung YS, Konofagou E. Permeability dependence study of the focused ultrasound-induced blood-brain barrier opening at distinct pressures and microbubble diameters using DCE-MRI. *Magn Reson Med* 2011;66:821-30.
30. Hynynen K, McDannold N, Vykhodtseva N et al. Focal disruption of the blood-brain barrier due to 260-kHz ultrasound bursts: a method for molecular imaging and targeted drug delivery. *J Neurosurg* 2006;105:445-54.
31. Hwang JH, Brayman AA, Reidy MA, Matula TJ, Kimmey MB, Crum LA. Vascular effects induced by combined 1-MHz ultrasound and microbubble contrast agent treatments in vivo. *Ultrasound Med Biol* 2005;31:553-64.
32. Ross JP, Cai X, Chiu JF, Yang J, Wu J. Optical and atomic force microscopic studies on sonoporation. *J Acoust Soc Am* 2002;111:1161-4.
33. Delalande A, Kotopoulis S, Postema M, Midoux P, Pichon C. Sonoporation: mechanistic insights and ongoing challenges for gene transfer. *Gene* 2013;525:191-9.
34. Chen H, Brayman AA, Bailey MR, Matula TJ. Blood vessel rupture by cavitation. *Urol Res* 2010;38:321-6.
35. Phenix CP, Togtema M, Pichardo S, Zehbe I, Curiel L. High intensity focused ultrasound technology, its scope and applications in therapy and drug delivery. *J Pharm Pharm Sci* 2014;17:136-53.
36. Manzoor AA, Lindner LH, Landon CD et al. Overcoming limitations in nanoparticle drug delivery: triggered, intravascular release to improve drug penetration into tumors. *Cancer Res* 2012;72:5566-75.
37. Suzuki R, Klivanov AL. Co-administration of Microbubbles and Drugs in Ultrasound-Assisted Drug Delivery: Comparison with Drug-Carrying Particles. *Adv Exp Med Biol* 2016;880:205-20.
38. Suzuki R, Maruyama K. Effective in vitro and in vivo gene delivery by the combination of liposomal bubbles (bubble liposomes) and ultrasound exposure. *Methods Mol Biol* 2010;605:473-86.
39. Ibsen S, Benchimol M, Simberg D, Esener S. Ultrasound mediated localized drug delivery. *Adv Exp Med Biol* 2012;733:145-53.
40. Afadzi M, Strand SP, Nilssen EA et al. Mechanisms of the ultrasound-mediated intracellular delivery of liposomes and dextrans. *IEEE Trans Ultrason Ferroelectr Freq Control* 2013;60:21-33.
41. Zhou Y, Kumon RE, Cui J, Deng CX. The size of sonoporation pores on the cell membrane. *Ultrasound Med Biol* 2009;35:1756-60.